sustainable chemistry

MDPI

Article

Green Synthesis of Sodium Cyanide Using Hydrogen Cyanide Extracted under Vacuum from Cassava (*Manihot esculenta* Crantz) Leaves

Ilunga Monga [1,2], Vimla Paul [1], Sudhakar Muniyasamy [3] and Orpah Zinyemba [2,*]

[1] Department of Chemistry, Durban University of Technology, 51-121 Steve Biko Rd, Musgrave, Berea 4001, South Africa; 20809093@dut4life.ac.za (I.M.); vimlap@dut.ac.za (V.P.)
[2] Department of Chemical Sciences, Auckland Park Kingsway Campus, University of Johannesburg, Auckland Park, Johannesburg 2006, South Africa
[3] Council for Scientific and Industrial Research (CSIR), Meiring Naudé Road, Brummeria, Pretoria 0001, South Africa; smuniyasamy@csir.co.za
* Correspondence: ozinyemba@uj.ac.za

Abstract: This study was carried out to develop a green approach to synthesising sodium cyanide (NaCN) using hydrogen cyanide (HCN) extracted from cassava (*Manihot esculenta* Crantz) leaves after 120 min of maceration at 30 °C and 45 min of recovery under vacuum at 35–40 °C. The CN^- ion released via autolysis was reacted with the Na^+ ion following vacuum extraction of the former to produce NaCN by saturating the absorbing sodium hydroxide (NaOH) solution. This specific extraction method avoided direct contact between the cassava leaves homogenate and the absorbing solution. NaCN was crystallised by drying the NaCN slurry at 100 °C in an air oven. A total of 15.70 kg of fresh cassava leaves was needed to produce 32.356 g of NaCN (green-NaCN) (% NaCN yield = 0.21%). The results of X-ray diffraction, attenuated total reflectance–Fourier transform infrared spectroscopy and scanning electron microscopy with energy-dispersive X-ray spectroscopy, show that NaCN was successfully prepared using the proposed method. These spectral techniques showed that the control and green-NaCN contained sodium carbonate impurities. The latter was quantified by the titration experiments and was found to be 0.61% and 2.29% in the control and green-NaCN, respectively. Furthermore, the titration experiments revealed that the residual NaOH content was 1.63% in control NaCN and 4.68% in green-NaCN. The aim of modifying the green synthesis route for producing NaCN from cassava, developed by the Attahdaniel research group in 2013 and 2020, was achieved.

Keywords: green synthesis; sodium cyanide; hydrogen cyanide; cassava; cyanogenic glucoside; linamarin

Citation: Monga, I.; Paul, V.; Muniyasamy, S.; Zinyemba, O. Green Synthesis of Sodium Cyanide Using Hydrogen Cyanide Extracted under Vacuum from Cassava (*Manihot esculenta* Crantz) Leaves. *Sustain. Chem.* **2022**, *3*, 312–333. https://doi.org/10.3390/suschem3030020

Academic Editors: Valeria La Parola and Leonarda Francesca Liotta

Received: 4 May 2022
Accepted: 10 June 2022
Published: 5 July 2022

1. Introduction

Sodium cyanide (NaCN) is a hygroscopic white crystalline or granular powder that releases a very toxic gas (hydrogen cyanide, HCN) when contacted with acids [1]. Industrially, NaCN was first produced by the Castner process, which is based on the reaction between sodium metal, charcoal and ammonia [1,2], as shown in Scheme 1:

$$\underset{\text{Sodium}}{2\,Na} + \underset{\text{Charcoal}}{2\,C} + \underset{\text{Ammonia}}{2\,NH_3} \longrightarrow \underset{\text{Sodium cyanide}}{2\,NaCN} + \underset{\text{Hydrogen}}{3\,H_2}$$

Scheme 1. Preparation of sodium cyanide via the Castner process.

Currently, it is manufactured exclusively by the neutralisation or wet process. This process involves the reaction of sodium hydroxide (NaOH) and liquid or gaseous HCN, as shown in Scheme 2 [1,2]:

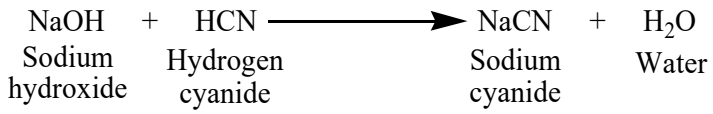

Scheme 2. Preparation of sodium cyanide via the neutralisation process.

Hydrogen cyanide (hydrocyanic acid or prussic acid), a clear poisonous liquid or gas, can be directly or indirectly prepared. It was first prepared in solution by Scheele in 1782 [3]. HCN can be produced when enough energy is supplied to any system containing carbon, hydrogen and nitrogen [3] using one of the following processes:

1.1. Direct Synthesis of HCN

1.1.1. Andrussow Process

According to Scheme 3, this widely used method, created around 1930, involves the reaction between methane, ammonia and air over platinum metals used as catalysts [1,3].

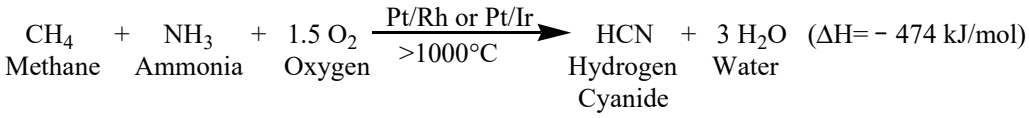

Scheme 3. Preparation of hydrogen cyanide via the Andrussow process.

1.1.2. Methane–Ammonia Process or Blausaure Methane Anlage (BMA)

HCN is prepared by reacting methane and ammonia in the absence of oxygen [1,3], as shown in Scheme 4.

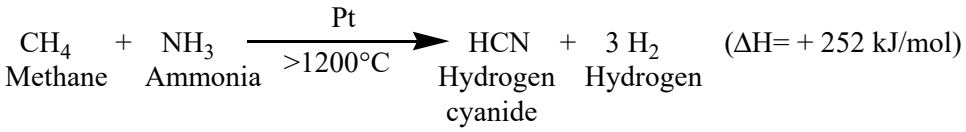

Scheme 4. Preparation of hydrogen cyanide via the BMA process.

1.1.3. Shawinigan Process

This HCN production method, developed in 1960, is also called the Fluohmic process. HCN is prepared by reacting hydrocarbon gases (mainly propane) with ammonia in an electrically heated fluidised bed of coke and in the absence of catalysts [1,3], as shown in Scheme 5.

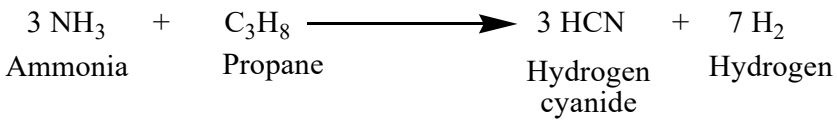

Scheme 5. Preparation of hydrogen cyanide via the Shawinigan process.

1.2. Indirect Synthesis of HCN

Sohio Process

HCN is produced as a by-product of the manufacturing of acrylonitrile during the reaction of propene and ammonia [1,4] according to Scheme 6.

Main reaction

$$2\,C_3H_6 + 2\,NH_3 + O_2 \longrightarrow 2\,C_3H_3N + 6\,H_2O$$

Propene Ammonia Oxygen Acrylonitrile Water

Side reactions

$$2\,C_3H_6 + 3\,NH_3 + 3\,O_2 \longrightarrow 3\,C_2H_3N + 6\,H_2O$$

Propene Ammonia Oxygen Acetonitrile Water

$$C_3H_6 + 3\,NH_3 + 3\,O_2 \longrightarrow 3\,HCN + 6\,H_2O$$

Propene Ammonia Oxygen Hydrogen cyanide Water

$$2\,C_3H_6 + 9\,O_2 \longrightarrow 6\,CO_2 + 6\,H_2O$$

Propene Oxygen Carbon dioxide Water

Scheme 6. Preparation of hydrogen cyanide (by-product) via the Sohio process.

From environmental management and sustainable perspectives, it is crucial to find alternative routes for the production of HCN to reduce the global energy and environmental problems associated with the use of hydrocarbons.

For this reason, since HCN is also known to naturally occur [3], further research was conducted by [2] and [5] to develop a green way to produce NaCN from cassava. The significant difference between these two studies is the method used to release HCN from cassava. In the study done by [2], HCN was released by the acid hydrolysis method, while the direct hydrolysis method was used in the study done by [5]. In both studies, the cassava extract was directly contacted with a 3.6 mol/L NaOH absorbing solution to form NaCN.

HCN is naturally produced by several organisms, such as bacteria, algae, fungi, plants [6,7], and some animals [6,8]. These organisms release HCN through the cyanogenic process as a defensive and offensive mechanism [7]. Plants are the primary natural source of HCN, with more than 2000 species producing it as cyanogenic glycosides (CNGs) [9,10].

Cassava, a staple food for more than half a billion people [5,11,12], is such a plant [13]. Cassava (*Manihot esculenta* Crantz), also called manioc or yuca [14], originated from Latin America. Although Portuguese merchants introduced it into western Africa in the 16th century [15,16], it became a staple food that was widely cultivated across the African continent in the middle of the 19th century [16]. Cassava was introduced in South Africa (SA) in the 1830s and 1860s during the Tsonga tribe's migrations. The Tsonga tribes adopted cassava as a food crop following its introduction into Mozambique by the Portuguese in the 17th century. Their migration routes took them westwards into Mpumalanga province (old Eastern Transvaal) and Swaziland, southwards into the North of KwaZulu-Natal province [17–19].

The two CNGs found in cassava, linamarin (93%) and lotaustralin (7%) [20,21], are called cyanogenic glucosides, since the cyano group is attached to a glucose molecule (Figure 1).

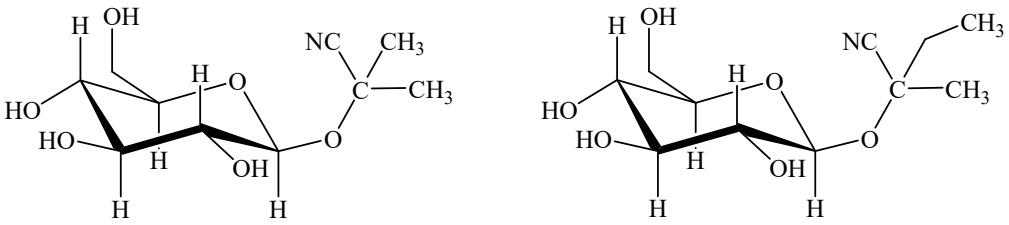

Figure 1. Structures of cyanogenic glucosides found in cassava.

HCN is produced following the release of hydrolytic enzymes during either the maceration of plant tissues or ingestion by the gut microflora [13], according to the reaction shown in Scheme 7:

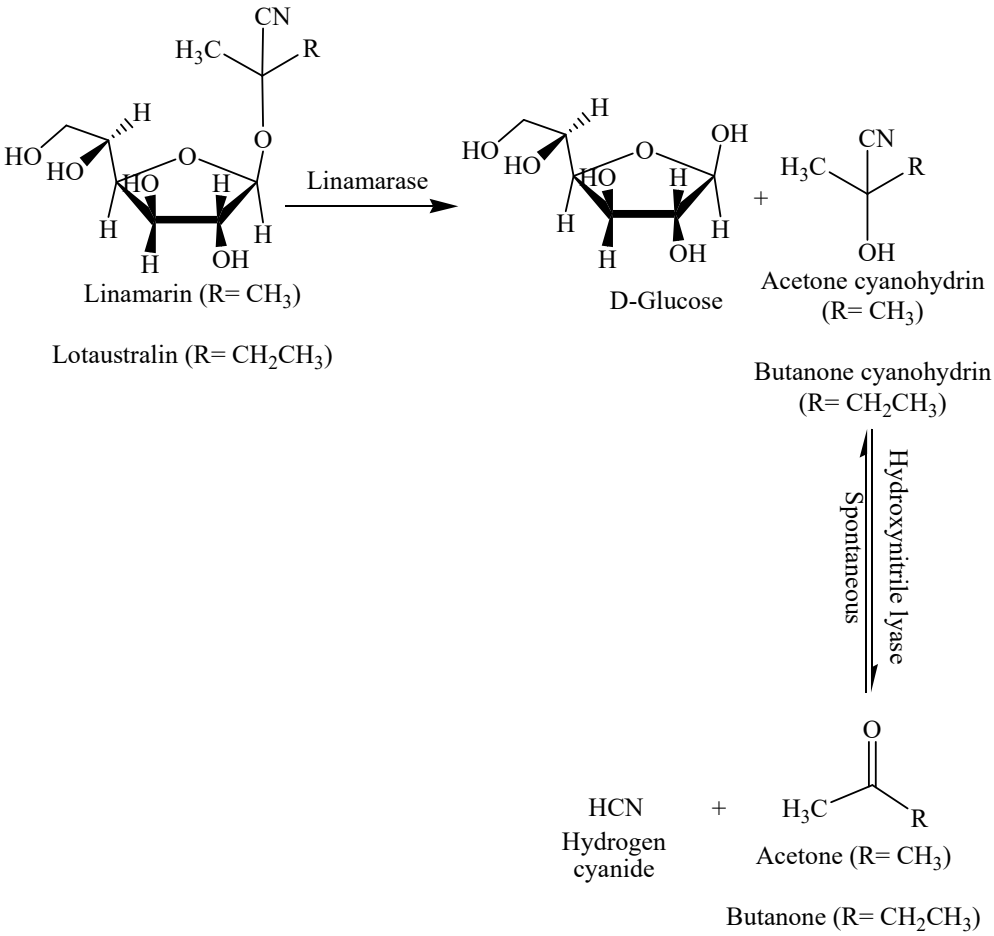

Scheme 7. Hydrolysis of cyanogenic glucoside (cyanogenesis).

This study extracted the HCN released from cassava leaves under vacuum at 35–40 °C, and then trapped it in a 3.6 mol/L NaOH absorbing solution to prepare NaCN. This extraction method was chosen as a competitive method to the ones used by [2] and [5] to prepare NaCN salt. The method developed in this study allowed the preparation of NaCN salt (green-NaCN) devoid of any plant contaminants arising from the direct contact between the plant homogenate and the absorbing solution.

2. Materials and Methods

2.1. Materials

2.1.1. Sample Collection

Fresh cassava leaves were purchased in Johannesburg, South Africa.

2.1.2. Chemicals

Chemicals used: 37% hydrochloric acid (HCl), 95% sodium cyanide * (NaCN, Product No 205222/Sigma-Aldrich, Johannesburg, South Africa), 99.5% sodium carbonate (Na_2CO_3, Product No 222321/Sigma-Aldrich, Johannesburg, South Africa), moist picric acid **, sodium hydroxide (NaOH), 95% sulphuric acid (H_2SO_4), Milli-Q water, phenolphthalein and methyl orange indicators.

Caution:

* Sodium cyanide and all other cyanides are deadly poisons, and extreme care must be taken in their use.

** Moist picric acid (2,4,6-Trinitrophenol) is dangerously explosive if it is allowed to dry out.

2.2. Methods

2.2.1. Optimisation of Maceration Time and Temperature and HCN Recovery Time

The cassava leaves samples (80 g of washed leaves grounded in 200 mL of cold Milli-Q water for 3 min) were macerated at different times (60, 120, 180 and 240 min) and temperatures (18 °C or room temperature, 30 °C and 37 °C) to determine the optimum conditions for autolysis to give the maximum amount of HCN. The optimal time for the HCN recovery under vacuum at 35–40 °C was also investigated after 30, 45 and 60 min of extraction.

The quantity of cassava leaves and Milli-Q water, given above, was tripled during the optimisation of the maceration temperature and quadrupled to optimise the other two parameters. The prepared homogenate was evenly divided into three or four portions before being subjected to the respective optimisation experiment. The four portions used to optimise the maceration time were macerated at 30 °C, while the ones used to optimise the % recovery of the released HCN were macerated at 30 °C for 120 min. Of the four homogenates prepared for the HCN recovery study, three were subjected to the optimisation process, and the fourth flask was used to determine the initial concentration. The three portions used to optimise the maceration temperature were macerated for 120 min. The liberated HCN was collected in 25 mL of a 3.6 mol/L solution. All optimisation experiments were done in quadruplicate.

The percentage (%) recovery of the released HCN was calculated as follows:

$$\%\ HCN\ recovered = \frac{Final\ (Average)\ HCN\ concentration}{Initial\ HCN\ concentration} \times 100\% \quad (1)$$

2.2.2. Sample Preparation

The sample preparation process is illustrated in Figure 2. A total of 250 g of washed cassava leaves were ground in a blender for 3 min in 1000 mL of cold Milli-Q water. Cold water was used to avoid the loss of the HCN gas released from the cassava leaves. The homogenate was immediately transferred to a stoppered distillation flask and macerated under optimum conditions.

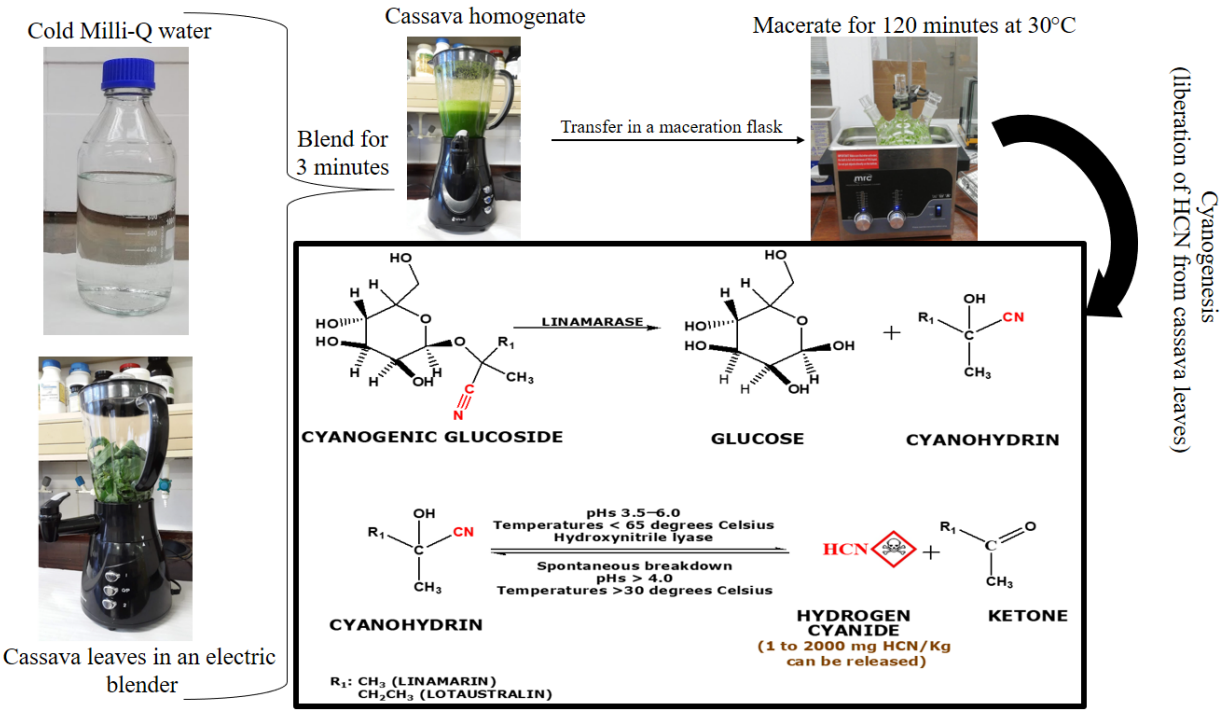

Figure 2. Preparation of cassava homogenate.

2.2.3. Saturation of 3.6 mol/L NaOH Solution

This process was achieved by connecting the flask containing the homogenate to a gas-tight system, as shown in Figure 3. The released HCN was recovered at 35–40 °C under a vacuum using optimum extraction conditions. Atmospheric air was used to agitate the homogenate and carry the liberated HCN into 250 mL of 3.6740 mol/L NaOH solution to form NaCN. Before reaching the homogenate flask, the air was passed through a carbon dioxide (CO_2) remover system. The CO_2 remover system consisted of five vessels mounted in series, containing 10 mol/L NaOH. The saturation of the 3.6 mol/L NaOH absorbing solution was done until the plateauing of the NaCN concentration occurred. The minimal change in the NaCN concentration caused the plateau formation observed during the saturation process.

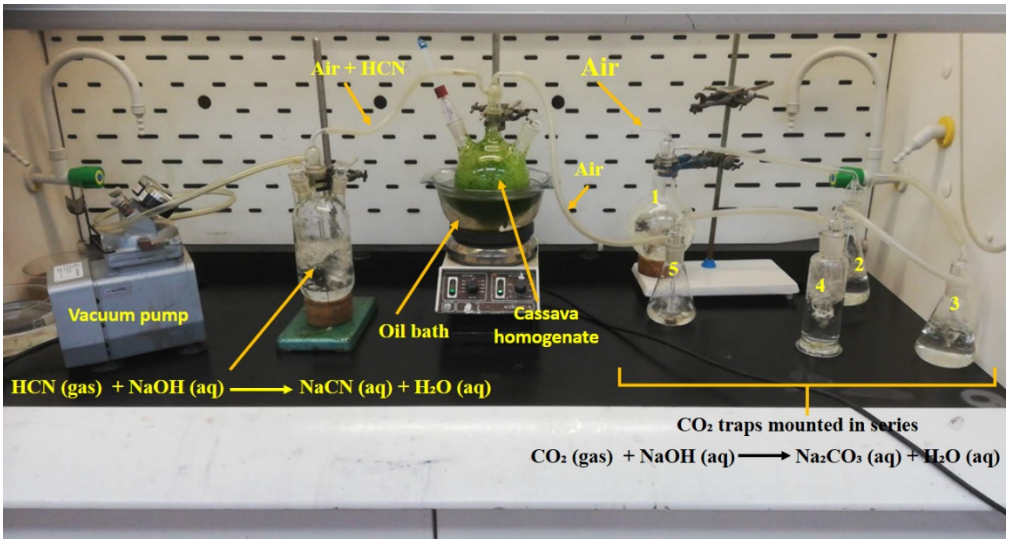

Figure 3. Recovery of hydrogen cyanide under vacuum at 35–40 °C.

2.2.4. Quantification of NaCN Solution

The alkaline picrate method, used to determine the concentrations of NaCN, is based on the reaction between the cyanide and alkaline picrate solution (prepared by mixing equal volumes of 2.56% picric acid and 5% sodium carbonate) [22], as shown in Scheme 8:

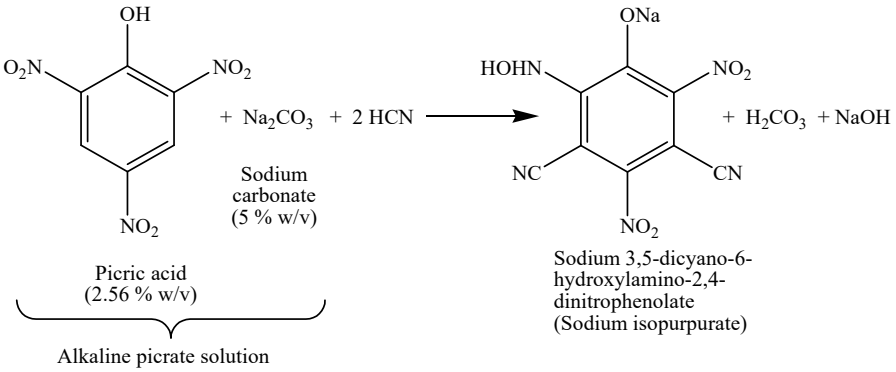

Scheme 8. Formation of sodium isopurpurate [23].

The cyanide concentration in the samples was determined after appropriate dilution. The absorbance of the HCN standard solutions, ranging from 0.5 to 10 µg HCN/mL, prepared with 0.01 mol/L sulphuric acid (H_2SO_4), was measured on a Shimadzu UV-1800 UV/Visible spectrometer at 485 nm. The results were used to draw the calibration curve, from which the cyanide content of the sample was extrapolated.

The sodium isopurpurate was formed by adding 2 mL of alkaline picrate solution to 2 mL of the standard and green-NaCN solutions. The resulting solutions were incubated for 15 min in a water bath set at 37 °C. A total of 15 µL of concentrated H_2SO_4 was added to the cold solutions to terminate the reaction and stabilise the readings before measurements were taken (Figure 4). The absorbances were measured against a blank containing only 0.01 mol/L H_2SO_4 and the alkaline picrate solution.

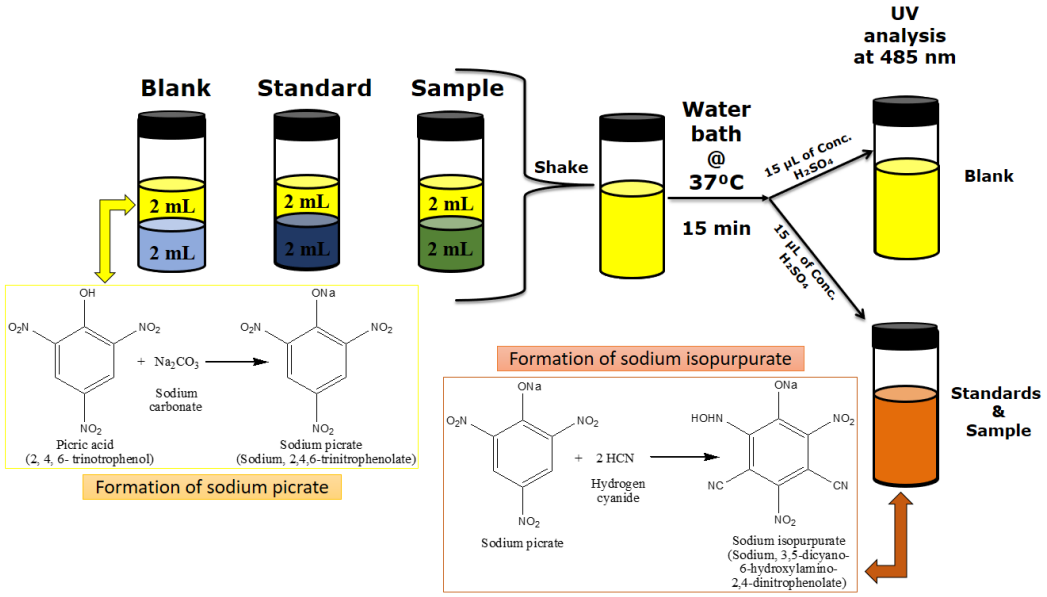

Figure 4. Samples preparation for UV analysis.

The concentration of the released HCN was calculated using the following equation:

$$HCN\left(\frac{mg}{kg}\right) = \frac{C \times V_m}{w} \quad (2)$$

Where C is the concentration in mg/L (the same as μg/mL) from the curve, V_m (L) is the volume of Milli-Q water used to macerate the sample, and W (kg) is the weight of the sample used to prepare the homogenate.

The concentration of NaCN (mol/L) was determined from the HCN concentration and the molecular weights (g/mol) of NaCN and HCN using the equation shown below:

$$\text{NaCN (mol/L)} = \frac{HCN\ \left(\frac{g}{L}\right) \times (Molecular\ weight\ of\ NaCN / Molecular\ weight\ of\ HCN)}{Molecular\ weight\ of\ NaCN} \quad (3)$$

2.2.5. Determination of Sodium Carbonate and Residual Sodium Hydroxide in Standard and Green-Sodium Cyanide Solutions

Sodium carbonate (Na_2CO_3) and residual sodium hydroxide (NaOH) were determined using the indicator method against a standardised 0.1 mol/L HCl solution. The complete neutralisation of NaOH and the half neutralisation of Na_2CO_3 were detected with phenolphthalein, while the neutralisation of the bicarbonate was detected with methyl orange.

2.2.6. Drying of Green-Sodium Cyanide Solution

The drying process was achieved following the steps described in Figure 5. The Na_2CO_3 present in the concentrated green-NaCN solution, obtained in step 1, was removed by the freezing-out carbonates method [24]. The NaCN concentrate was cooled to a temperature close to zero (1–4 °C) to remove Na_2CO_3 as a precipitate. The supernatant was removed after decantation and subjected to the rest of the drying process. The green-NaCN slurry and any precipitated Na_2CO_3 were dried in an oven at 100 °C.

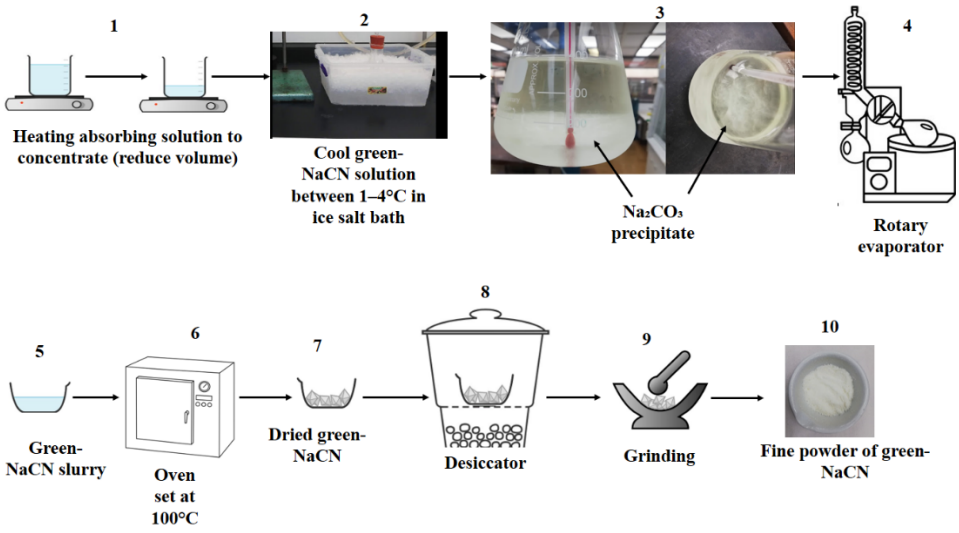

Figure 5. Steps of the drying process.

The percentage yield of green-NaCN was calculated as follows:

$$\%\ yield\ of\ NaCN = \frac{Mass\ of\ green\ NaCN}{Mass\ of\ cassava\ leaves} \times 100\% \quad (4)$$

2.2.7. Structural Confirmation of Synthesised Sodium Cyanide Salt

The identity, crystal structure and purity of the NaCN solid (green-NaCN), obtained as described in Section 2.2.6, were compared against a control sample (NaCN standard) by attenuated total reflectance–Fourier transform infrared spectroscopy (ATR–FTIR), powder X-ray diffraction analysis (XRD) and scanning electron microscopy with energy-dispersive X-ray spectroscopy (SEM/EDS).

- Attenuated total reflectance–Fourier transform infrared spectroscopy (ATR–FTIR)

The ATR–FTIR spectra of both the NaCN standard and green-NaCN were recorded in the wavenumber range of 4000–400 cm^{-1} on a Shimadzu QART-S single reflectance ATR accessory attached to an IR Spirit Shimadzu spectrophotometer. The precipitated Na_2CO_3 was also examined under the same parameters and compared against the control Na_2CO_3.

- X-ray diffraction analysis (XRD)

This technique determined the crystal structure and phase purity of finely crushed and homogeneous green-NaCN and precipitated Na_2CO_3. The XRD patterns were recorded at 25 °C and an angle of 2θ on a PANalytical X'Pert PRO X-ray diffractometer using CuKα radiation with a wavelength of 1.54060 Å. The PANalytical X'Pert Highscore software was used to analyse all samples in a range of 4.0124 to 89.9814°2θ with a step size of 0.0170°/step. The data were processed using the Match! Software (Version 3.8.2.148).

- Scanning electron microscopy with energy-dispersive X-ray spectroscopy (SEM-EDS)

SEM-EDS was used to examine the morphology and determine the elemental composition of finely crushed green-NaCN and precipitated Na_2CO_3 using the JEOL 7800F Field Emission Scanning Electron Microscope (FE-SEM).

3. Results and Discussion

3.1. Optimisation of Maceration Time and Temperature and Recovery Time for Maximum Release of Hydrogen Cyanide from Cassava Leaves

Figure 6 shows the concentration of the HCN released after 60, 120, 180 and 240 min of maceration. The HCN concentration increased with time. However, it is interesting to note that the increase in released HCN from 120 to 240 min is minimal, rather than the abrupt cyanide increase observed from 60 to 120 min. This trend was seen across the board in all replicate experiments.

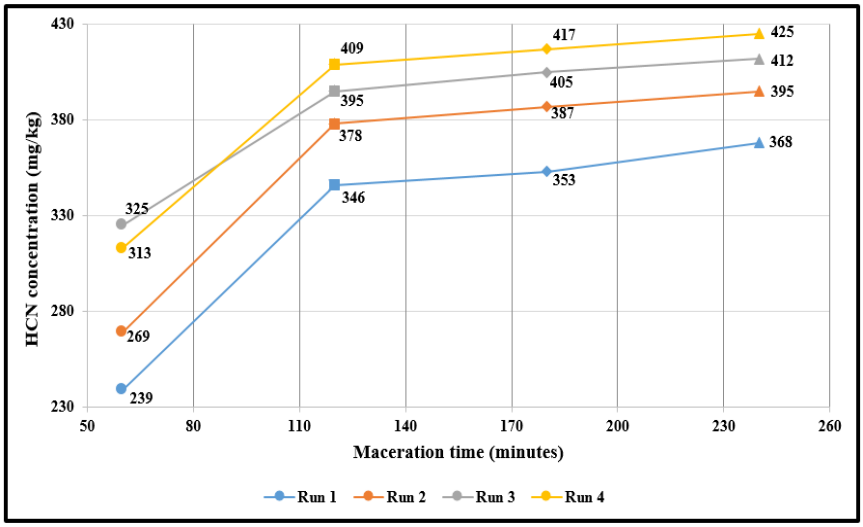

Figure 6. Concentrations of HCN (mg/kg) obtained after 45 min of extraction under vacuum at 35–40 °C and analysed, as depicted in Figure 4, after maceration (n = 4) of cassava leaves at 30 °C for different times (Symbols ●, ■, ♦, and ▲ represent maceration time of 60, 120, 180 and 240 min, respectively).

These findings are similar to the study results by [25]. According to this study, linseed was macerated for 120 to 240 min to release HCN. Therefore, since the increase in the HCN concentration was minimal in this range, 120 min of maceration time was used throughout the study.

Figure 7 shows the concentration of the HCN released after 120 min of maceration at 18 °C (room temperature), 30 °C and 37 °C. The HCN concentration increased from 18 to 30 °C before decreasing. All replicate experiments revealed the same trend. The decrease in

the HCN concentration could be explained by a reduction in enzymatic activities [26]. These results suggest that the optimum temperature for the maximum HCN release is 30 °C.

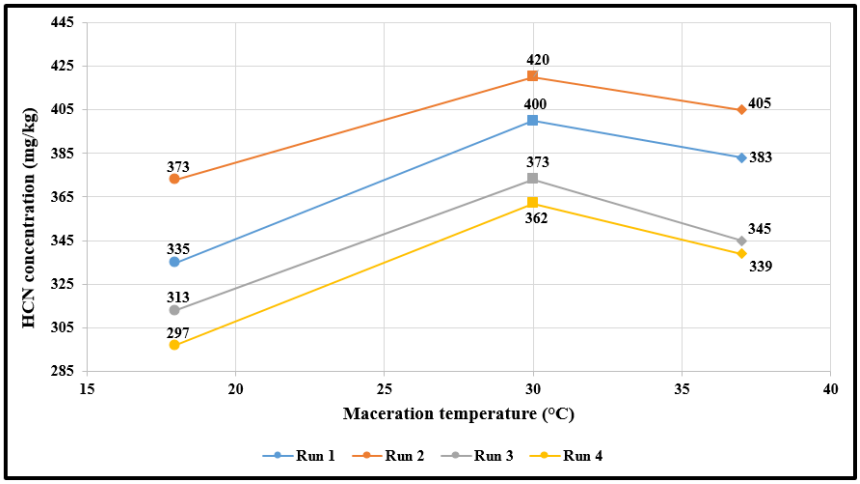

Figure 7. Concentrations of HCN (mg/kg) obtained after 45 min of extraction under vacuum at 35–40 °C and analysed, as depicted in Figure 4, after maceration (n = 4) of cassava leaves for 120 min at different temperatures (Symbols ●, ■, and ♦ represent maceration temperature of 18, 30 and 37 °C, respectively).

The concentrations of the HCN released after macerating the cassava leaves for 120 min at 30 °C and recovered after 30, 45 and 60 min of extraction under vacuum at 35–40 °C, are shown in Table 1. The experimental setup is depicted in Figure 8.

Table 1. The various concentrations, % recovered and % RSD values for HCN recovery from cassava leaves after 120 min of maceration (n = 4) at 30 °C and extraction under vacuum at 35–40 °C for 30, 45 and 60 min.

	Initial HCN concentration (mg/kg) *					
	Run 1	**Run 2**	**Run 3**	**Run 4**		
	581.40	784.86	414.01	317.96		
	Final/recovered HCN concentration (mg/kg)					
	Run 1	**Run 2**	**Run 3**	**Run 4**		
30 min extraction	574.19	756.18	406.24	309.98	**Average % recovered**	**% RSD**
Recovery (%)	**98.76**	**96.35**	**98.12**	**97.49**	**97.68**	**1.05**
45 min extraction	571.22	766.26	403.56	317.17	**Average % recovered**	**% RSD**
Recovery (%)	**98.25**	**97.63**	**97.47**	**99.75**	**98.28**	**1.06**
60 min extraction	568.38	761.29	394.72	305.62	**Average % recovered**	**% RSD**
Recovery (%)	**97.76**	**97.00**	**95.34**	**96.12**	**96.55**	**1.09**

* The cassava leaves used for each run did not come from the same batch.

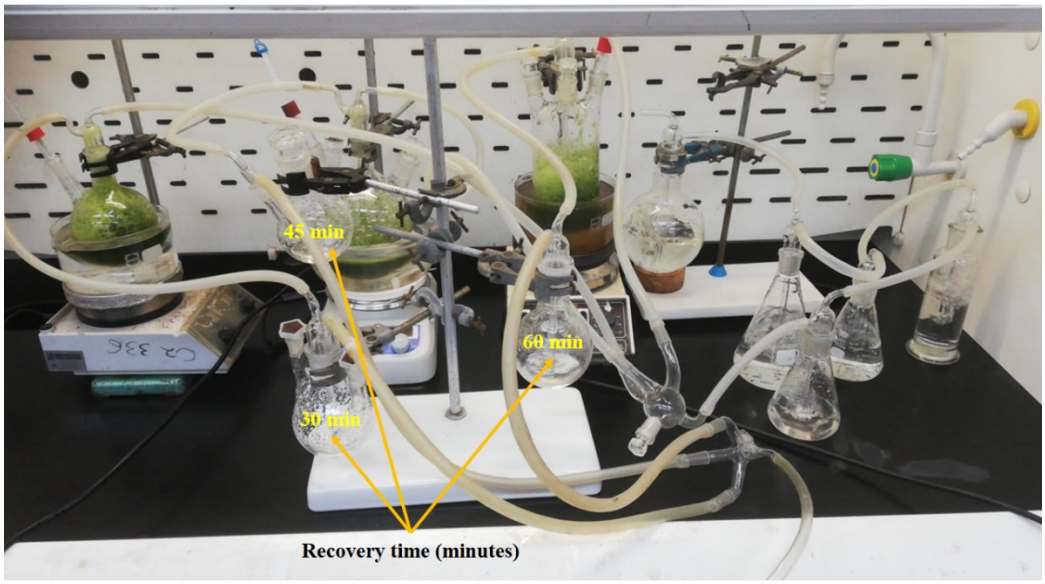

Figure 8. Experimental setup of the recovery study.

The percentage recoveries were 97.68 ± 1.03%, 98.28 ± 1.04% and 96.55 ± 1.05% after 30, 45 and 60 min of extraction, respectively, as shown in Figure 9. Irrespective of the cassava leaves batch used, the % recoveries were approximately the same at each extraction time and within the acceptable analytical range. These percentage recoveries were calculated using Equation (1). From these results, we can see that the maximum HCN recovery was achieved after 45 min of extraction.

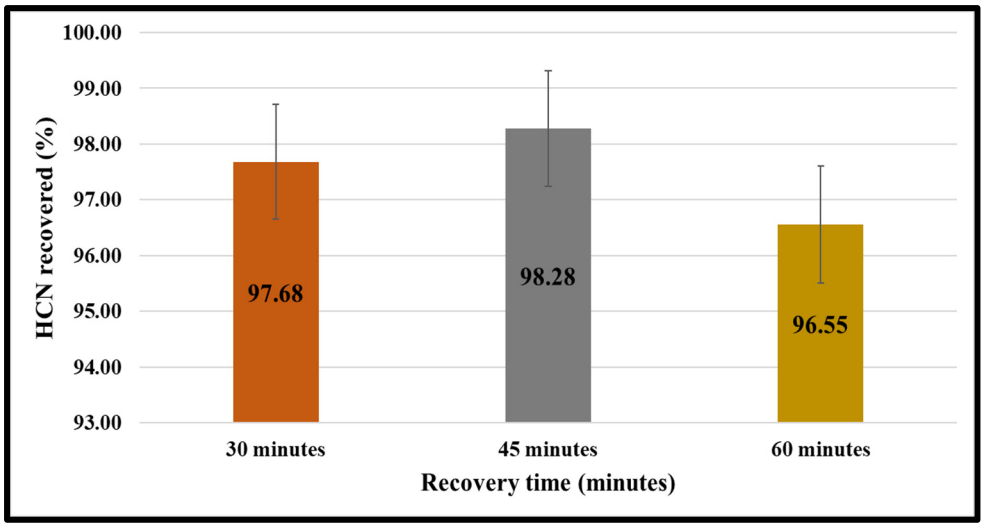

Figure 9. HCN recovered (%) at different times under vacuum at 35–40 °C after maceration (n = 4) of cassava leaves at 30 °C for 120 min.

Thus, the optimum conditions for the succeeding experiments were maceration at 30 °C for 120 min followed by 45 min of extraction under vacuum at 35–40 °C.

3.2. Saturation of 3.6740 mol/L Absorbing Solution

Figure 10 shows the saturation of 250 mL of the 3.6740 mol/L NaOH solution. This process was done using the optimum extractions conditions and continued until the plateauing of the NaCN concentration was observed.

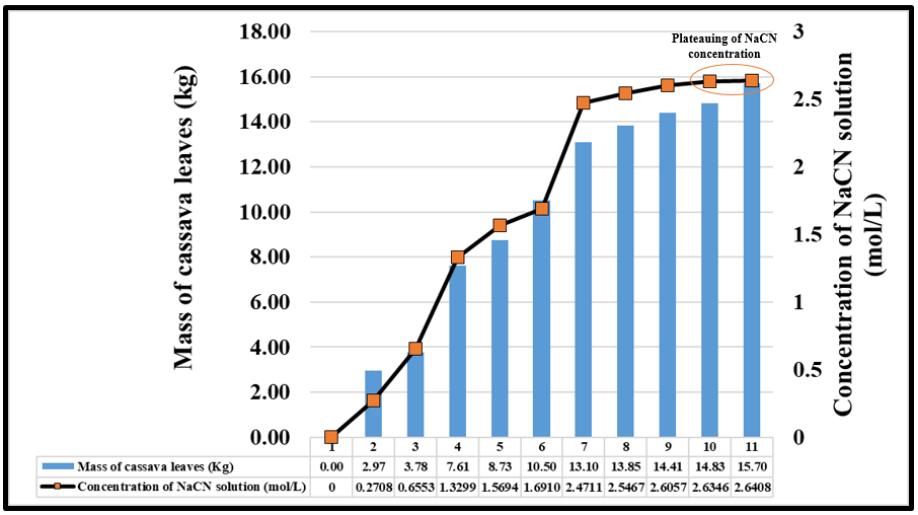

Figure 10. Preparation of NaCN solution by saturation of 3.6740 mol/L NaOH absorbing solution over time with HCN gas extracted for 45 min under vacuum at 35–40 °C from cassava leaves after 120 min of maceration at 30 °C.

From Figure 10, we see that 15.70 kg of fresh cassava leaves were used to saturate the absorbing solution with extracted HCN gas. This result suggests that the quantity of cassava leaves needed to saturate the absorbing solution solely depends on the concentration of the HCN liberated. Hence, the leaves used in this study had a low HCN content. The saturation process was stopped when the concentration of the prepared NaCN solution plateaued around 2.6 mol/L. Interestingly, the final NaCN concentration (2.6408 mol/L) was lower than the concentration of the absorbing solution (3.6740 mol/L). This result shows that the concentration of the absorbing solution and the amount of CO_2 absorbed from the atmosphere restrict the final concentration of NaCN. The former can be overcome by increasing the concentration of the absorbing solution, while the latter can be minimised by limiting the contact time between the absorbing solution and atmospheric CO_2.

The concentration of NaCN in the absorbing solution was extrapolated from a calibration curve, as shown in Figure 11, generated using the method described in Section 2.2.4. The colour intensity of the sodium isopurpurate is directly proportional to the amount of cyanide present in the samples (Figure 12). This process was repeated with fresh reagents until saturation was complete.

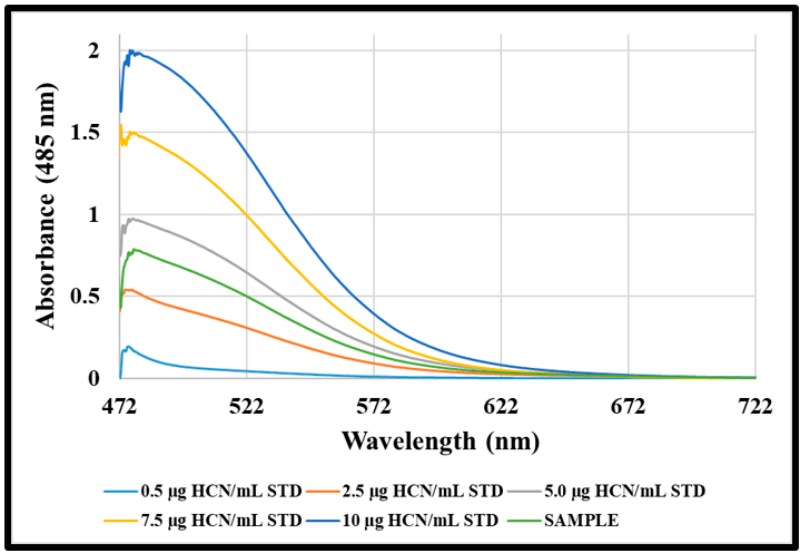

Figure 11. Typical standard calibration curve for spectrophotometric determination of HCN.

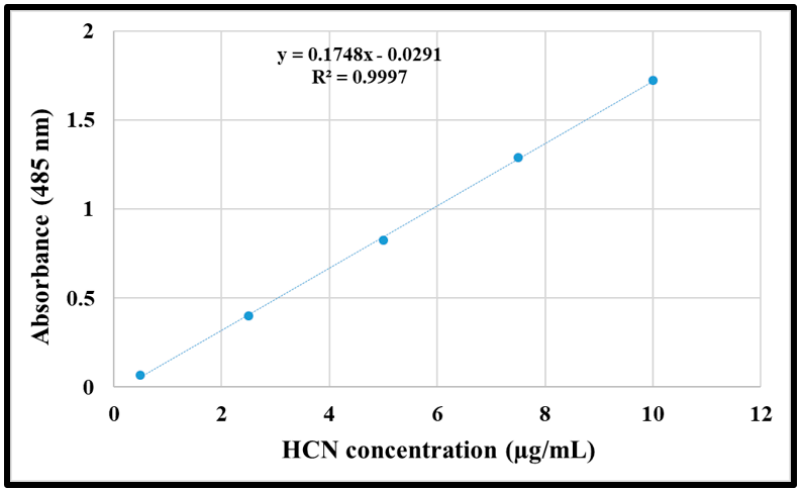

Figure 12. Typical absorption spectra of cyanide standards and the sample obtained from the proposed method.

3.3. Estimation of Sodium Carbonate and Residual Sodium Hydroxide in Standard and Green-Sodium Cyanide Salts

Table 2 shows the titration results, and the amounts of sodium carbonate (Na_2CO_3) and residual sodium hydroxide (NaOH) contained in the standard and green-NaCN salts. Na_2CO_3 is found in both NaCN salts and originates from the reaction between the atmospheric CO_2 and the absorbing solution during the neutralisation and drying processes.

Table 2. Estimation of Na_2CO_3 and residual NaOH in standard and green-NaCN.

Sample Aliquot (mL)	Burette Reading (mL)			Titrant Used for NaOH and Half of Na_2CO_3 (mL)	Titrant Used for NaOH and Na_2CO_3 (mL)	Titrant Used for HCO_3^- (mL)	Titrant Used for Na_2CO_3 (mL)	Titrant Used for NaOH (mL)
	Initial Volume	1st Endpoint	2nd Endpoint					
	V_1	V_2	V_3	$V_4 = (V_2 - V_1)$	$V_5 = (V_3 - V_1)$	$V_6 = (V_5 - V_4)$	$V_a = 2V_6$	$V_b = (V_5 - 2V_6)$
Titration of 2.6408 mol/L control NaCN solution								
25	0.00	4.47 ± 0.01	5.00 ± 0.01	4.47 ± 0.01	5.00 ± 0.01	0.53 ± 0.00	1.05 ± 0.01	3.95 ± 0.01
Titration of 2.6408 mol/L green-NaCN solution								
25	0.00	17.52 ± 0.02	20.25 ± 0.02	17.52 ± 0.02	20.25 ± 0.02	2.74 ± 0.01	5.47 ± 0.02	14.78 ± 0.02
Estimation of Na_2CO_3 and residual NaOH								
					Na_2CO_3		**Residual NaOH**	
					Control NaCN solution	**Green-NaCN solution**	**Control NaCN solution**	**Green-NaCN solution**
Molarity (mol/L)					0.05746	0.2165	0.4323	1.1699
Strength (g/L)					6.0902	22.9468	17.2920	46.7960
Percentage (% *w/v*)					0.61	2.29	1.73	4.68

The Na_2CO_3 and residual NaOH contents were 0.61% and 1.73% in the control NaCN sample and 2.29% and 4.68% in green-NaCN. The results obtained from the green-NaCN reveal the presence of a substantial amount of NaOH after the saturation process. Hence, since NaOH readily reacts with atmospheric CO_2 to form Na_2CO_3, it is advisable to continue saturation well past the onset of plateauing of the NaCN concentration to decrease the concentration of unreacted NaOH. The Na_2CO_3 present in the NaCN salts could have been formed during the preparation of the NaOH absorbing solution and the latter's handling during the saturation process when it came into contact with atmospheric CO_2. However, Na_2CO_3 is also present in commercial NaCN, devoid of any residual NaOH from its reaction with the product formed by atmospheric CO_2 and water (H_2O). Hence, NaCN salt must always be stored in a tightly-closed container to avoid contact with atmospheric CO_2.

3.4. Structural Characterisation of Sodium Cyanide Salt

A total of 32.356 g of NaCN salt (green-NaCN) was obtained after drying the green-NaCN solution according to the method described in Section 2.2.6. The percentage yield of the green-NaCN prepared from cassava leaves was determined using Equation (4):

$$\%\ yield\ green - NaCN = \frac{32.356\ g}{15.70 \times 10^3\ g} \times 100\% = 0.21\%$$

The yield obtained from the cassava leaves, using the proposed method, was very low as compared to the values obtained by [2] and [5] (Table 3).

Table 3. The % yield of NaCN salt obtained from different cassava samples.

Cassava Sample							Method Used to Extract Cyanogenic Glucosides	Reference
Fresh Leaves	**Fresh Peels**	**Fresh Tuber Tissue**	**Fresh Whole Tuber Tissue**	**Dried Leaves**	**Dried Peels**	**Dried Whole Tuber**		
5.68	5.50	5.90	5.27	4.61	4.27	5.11	Acid hydrolysis	[2]
-	10.08	10.06	9.46	-	-	-	Acid hydrolysis	[5]
-	5.50	5.86	3.92	-	-	-	Direct hydrolysis (Deionised water)	
0.21	-	-	-	-	-	-	Direct hydrolysis (Deionised water)	This study

The low yield that was obtained in this study could be due to the low HCN content of the cassava leaves variety used. The low yield can be overcome using the cassava variety or other cyanogenic plants with high HCN contents.

The identity, crystal structure and purity of green-NaCN and precipitated Na_2CO_3 were confirmed against control NaCN and control Na_2CO_3.

3.4.1. Attenuated Total Reflectance–Fourier Transform Infrared Spectroscopy (ATR–FTIR)

The ATR–FTIR spectra and the characteristic peaks of control NaCN and green-NaCN are given in Figure 13. Both spectra show a small, sharp O-H stretching peak at 2970 cm^{-1} due to water absorption. They exhibited a characteristic sharp, high-intensity peak at 2090 cm^{-1}, corresponding to the C≡N stretching vibration, observed in inorganic cyanide [27]. The O-H bending is displayed at 1738 cm^{-1} by both samples and at 1594 and 1607 cm^{-1} by the control NaCN and green-NaCN, respectively. These peaks appeared from the vapour phase of water.

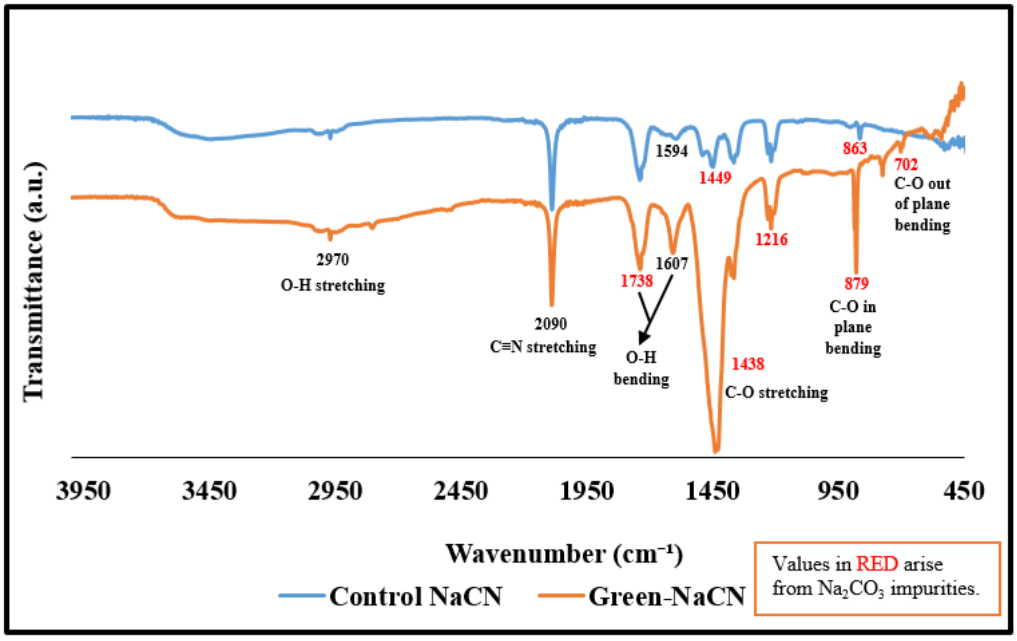

Figure 13. ATR–FTIR spectra of sodium cyanide (NaCN).

The IR spectra of both NaCN samples also revealed the presence of bands specific to the carbonate group. It is to be expected, since the formation of the latter arises from the reaction between atmospheric CO_2 and (I) NaOH during the preparation of NaCN by the neutralisation method; (II) the unreacted NaOH during the drying of NaCN slurry in an air oven; (III) atmospheric H_2O to form carbonic acid (H_2CO_3), which will react with pure NaCN (free of residual NaOH) to give sodium bicarbonate ($NaHCO_3$), Na_2CO_3 and HCN in equilibria. If HCN is released, the equilibrium would shift. The C-O stretching peak, and C-O in-plane and out-of-plane bending peaks were, respectively, observed at 1449 cm^{-1}, 863 cm^{-1} and 686 cm^{-1} in the IR spectrum of control NaCN.

The observed intense broadband at 1438 cm^{-1} was attributed to C-O stretching. The narrow sharp bands at 879 cm^{-1} and 702 cm^{-1}, corresponding to C-O in-plane and out-of-plane bending, were observed in the spectrum of green-NaCN. The IR spectrum, shown in Figure 12, also revealed that green-NaCN has more Na_2CO_3 impurity than the control sample. These findings further support the titration results displayed in Table 2.

Figure 14 shows the ATR–FTIR spectra of the control Na_2CO_3 and precipitated Na_2CO_3. A small, broad peak at 1738 cm^{-1}, resulting from the vapour phase of water, was observed on the spectrum of the control sample. C-O stretching gave rise to the intense, broad absorption band observed at 1421 cm^{-1}. C-O in-plane and out-of-plane bending gave the narrow sharp bands at 878 cm^{-1} and 702 cm^{-1}. Similar peaks, except for the small, broad peak at 3575 cm^{-1}, caused by the vapour phase of water, and the narrow peak at 2970 cm^{-1}, caused by water absorption by the sample, were observed on the spectrum of precipitated Na_2CO_3.

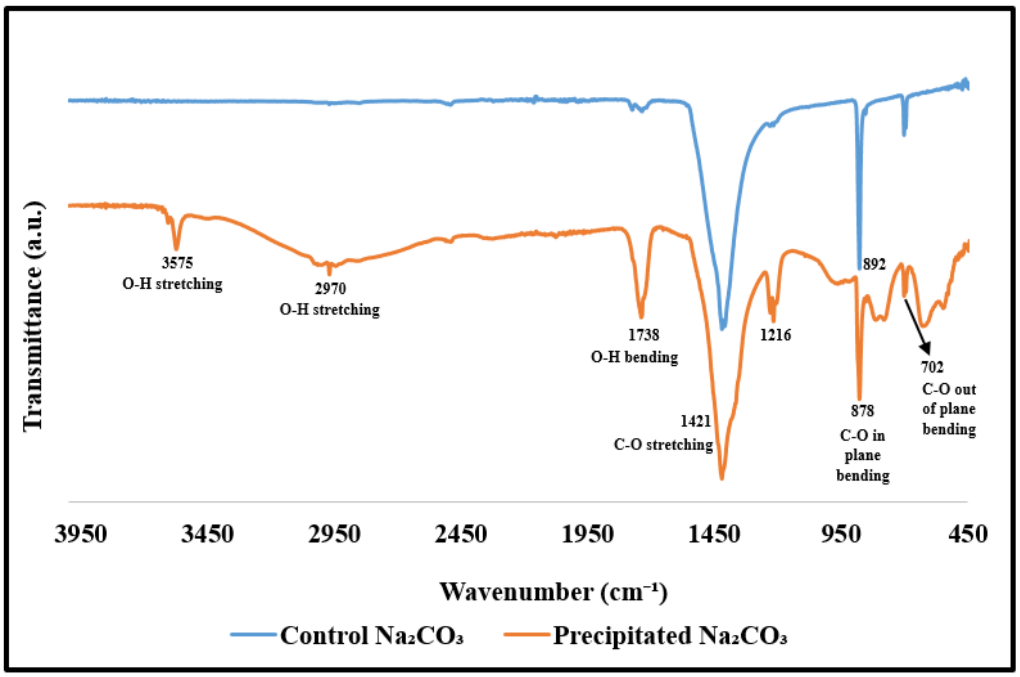

Figure 14. ATR–FTIR spectra of sodium carbonate (Na_2CO_3).

3.4.2. X-ray Diffraction (XRD)

The XRD spectra were generated using the Match! 3 software. It allowed us to identify the different phases present in the NaCN and Na_2CO_3 samples. The quantitative phase analysis was done using the Rietveld analysis. Although the R Bragg average values were high, the quality fits that gave the best difference plots are displayed in Figures 15 and 16.

The X-ray diffraction patterns of control NaCN and green-NaCN, recorded at 2θ angles, are shown in Figure 15. Control NaCN (a) and green-NaCN (b) showed similar XRD patterns at (30.3622°, 30.4557°); (34.1697°, 34.3051°); (38.6422°, 38.5661°); (43.4601°, 43.5524°); (51.4398°, 51.5940°); (53.9323°, 54.0450°); (63.1456°, 63.2228°) and (71.6529°, 71.,7345°), respectively. The control NaCN phase strongly matched the sodium cyanide reference phase, ICDD 00-030-1187 (Sodium cyanide hydrate). The green-NaCN phase matched the sodium cyanide reference phase, ICDD 00-037-1490 (Sodium cyanide). The amount of NaCN was 93.1% in the control sample and 76.5% in the green-NaCN. In addition, the XRD pattern of green-NaCN confirmed that the synthesised NaCN had more carbonates (8.8% of Na_2CO_3 and 14.5% of $NaHCO_3$) than the control sample, which only had 4.9% of Na_2CO_3 and 1.9% of $NaHCO_3$. The sodium carbonate present in green-NaCN was matched to the reference phase, ICDD 00-037-0451 (Sodium carbonate). Both NaCN samples contained trace levels of NaOH (0.1% in the control sample and 0.2% in green-NaCN). These results further confirm the presence of Na_2CO_3, identified by NaCN ATR–FTIR and titration, as shown in Figure 12 and Table 2, respectively. The discrepancy in Na_2CO_3 and the NaOH concentration could have been caused by human error during titration, or the quality of fit during the Rietveld refinement fitting.

The visual inspection of the patterns displayed in Figure 15 indicates that the green-NaCN crystals are smaller than the ones from the control sample.

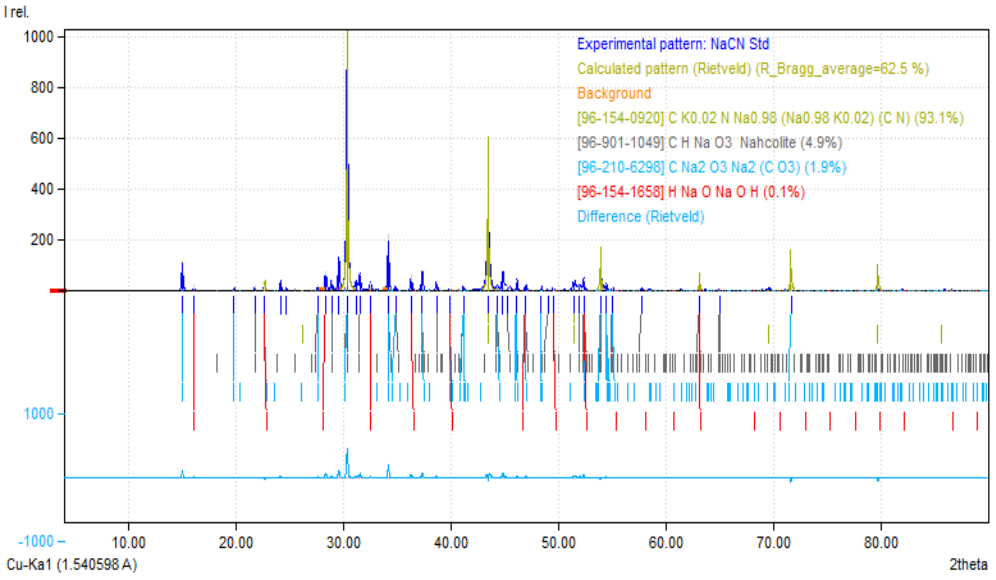

(**a**)

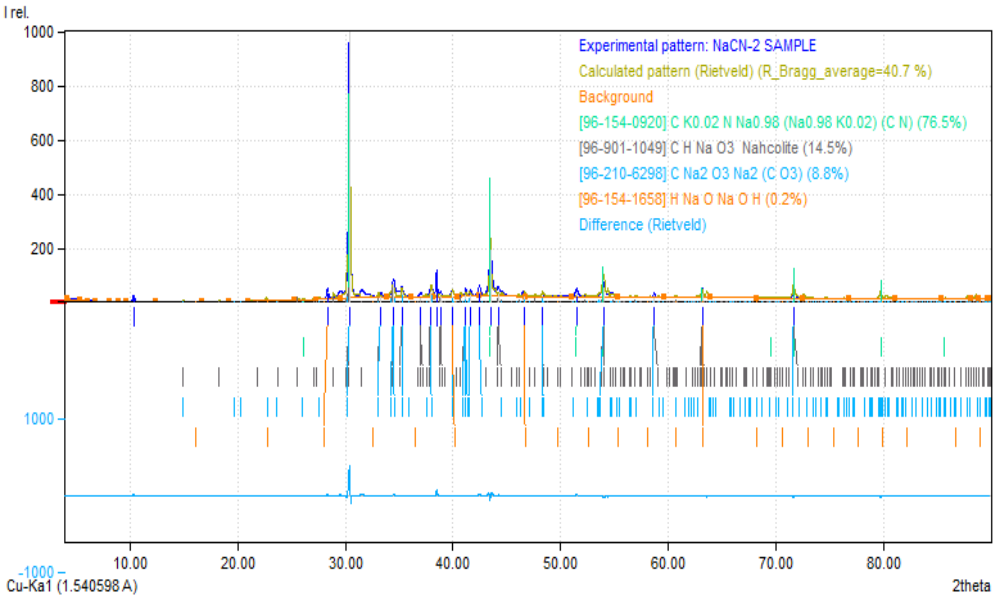

(**b**)

Figure 15. X-ray diffraction patterns of (**a**) control NaCN and (**b**) green-NaCN.

Figure 16 shows the XRD patterns of control Na_2CO_3 (a) and precipitated Na_2CO_3 (b) removed from the NaCN concentrated solution according to the method described in Section 2.2.6. The majority of peaks observed on the XRD pattern of precipitated Na_2CO_3 were similar to those appearing on the XRD pattern of the control sample. The following peaks from the control sample and precipitated Na_2CO_3 XRD patterns at 2θ angles are the ones with a noticeable intensity: (26.0488°, 26.1171°); (27.6403°, 27.6929°); (30.1267°, 30.2095°); (33.0273°, 33.1090°); (34.1899°, 34.2551°); (34.5083°, 34.5967°); (35.2238°, 35.2897°); (37.9650°, 38.0721°); (41.0923°, 41.1613°); (41.4807°, 41.5597°); (46.5246°, 46.6025°); (48.2568°, 48.3199°); (53.5670°, 53.6561°); (72.2691°, 72.0894°); (74.4908°, 74.5749°) and (80.3060°, 80.4246°), respectively. The control Na_2CO_3 phase strongly matched the sodium carbonate reference phase, ICDD 04-011-4108 (Sodium carbonate - Natrite), while the precipitated Na_2CO_3 was a strong match to the sodium carbonate reference phase, ICDD 05-001-0022 (Sodium carbonate -γ-form). In the control and precipitated samples, the carbonates were

88.1% and 90.9% of Na_2CO_3 and 11.5% and 7.7% of $NaHCO_3$, respectively. Trace levels of NaOH were also found in the control sample (0.4%) and the precipitated sample (0.3%). The precipitated sample had 1.1% of NaCN. It originated from the residual green-NaCN solution remaining during the drying process (see Section 2.2.6). Both the green-NaCN and the precipitated Na_2CO_3 were found to be crystalline, with the former exhibiting a cubic crystal structure [28], while the latter had a monoclinic crystal structure.

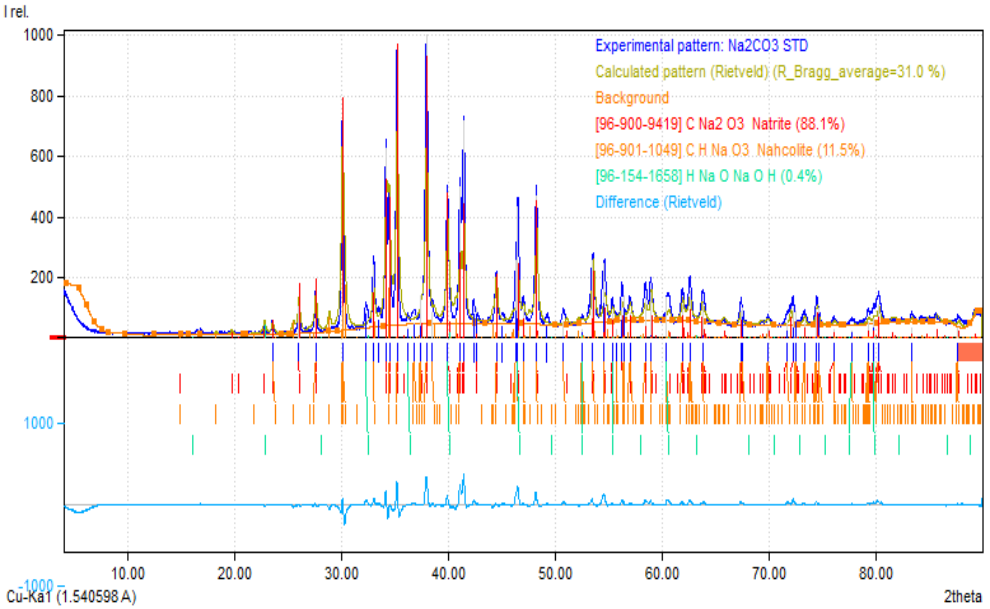

(**a**)

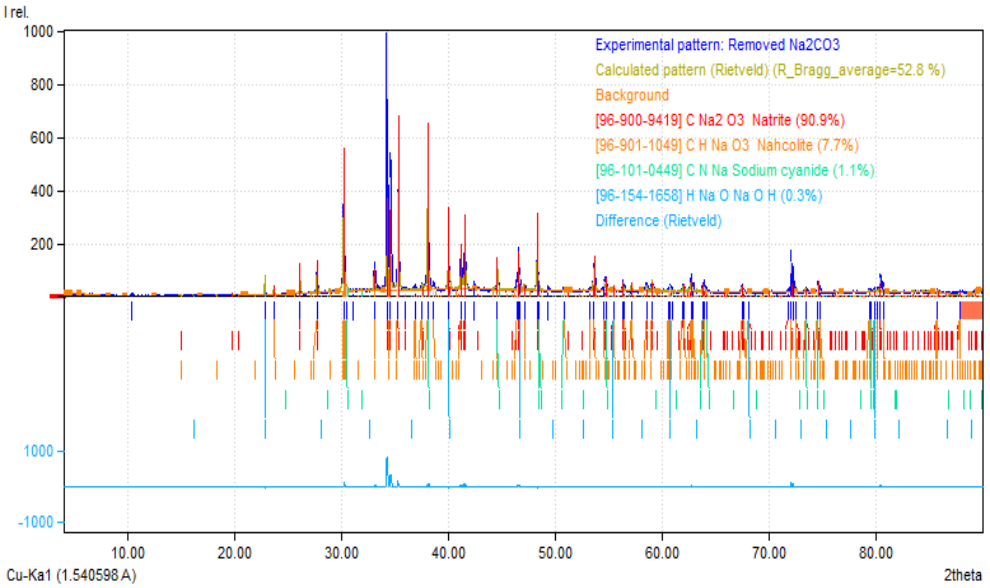

(**b**)

Figure 16. X-ray diffraction patterns of (**a**) control Na_2CO_3 and (**b**) precipitated Na_2CO_3.

3.4.3. Scanning Electron Microscopy with Energy-Dispersive X-ray Spectroscopy (SEM-EDS)

The ideal morphology of NaCN and Na_2CO_3 crystal is cubic and monoclinic, respectively. Figure 17 shows the morphology of control NaCN (a) and the product synthesised in this study (green-NaCN (b)). As can be seen, both control NaCN (Figure 17a) and green-NaCN (Figure 17b) exhibited a cubic shape with some monoclinic shape due to

Na_2CO_3. The control Na_2CO_3 (Figure 18a) and precipitated Na_2CO_3 (Figure 18b), removed from the concentrated NaCN solution, were monoclinic. These results complement and confirm the findings of the ATR–FTIR and XRD analyses.

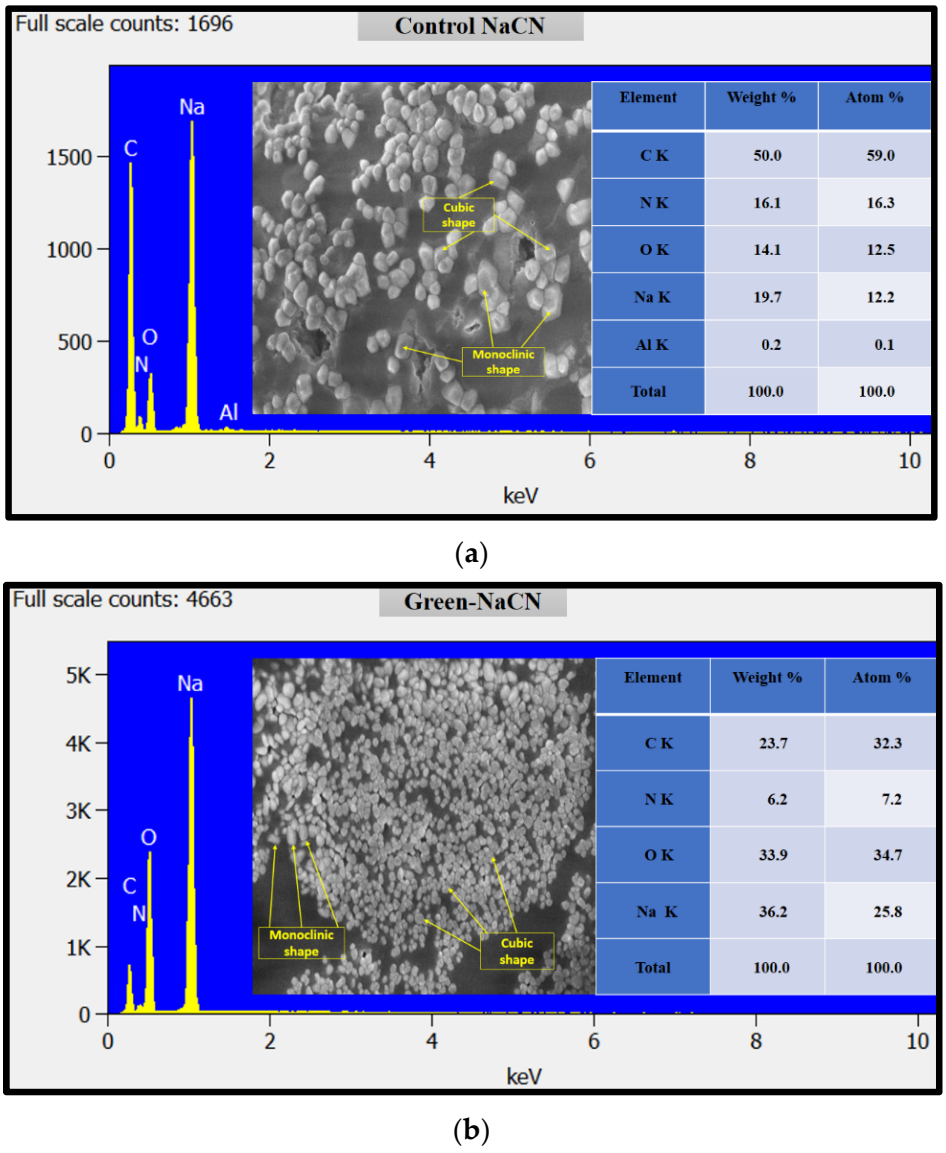

Figure 17. SEM images and EDS spectra of (**a**) control NaCN and (**b**) green-NaCN.

The EDS analysis was performed on synthesised salt to validate the production of NaCN by the suggested technique. Both NaCN and Na_2CO_3 were observed in the synthesised sample according to the EDS spectrum in Figure 17b. The same findings were obtained in the control sample (Figure 17a). In green-NaCN, the atomic percentages of sodium (Na), carbon (C), nitrogen (N), and oxygen (O) were 25.8, 32.3, 7.2, and 34.7, respectively. In control NaCN, their atomic % amounts were 12.2, 59.0, 16.3, and 12.5. There was also a negligible amount of aluminium impurities (0.1 atomic %) in the control NaCN. The spectra in Figure 17 also show that the NaCN crystals in the green-NaCN sample are smaller than in the control sample. Na, C, and O were found in 28.3, 31.9, and 39.8 atomic %, respectively, in the EDS spectra of precipitated Na_2CO_3 (Figure 18a). The EDS spectra of the control Na_2CO_3 (Figure 18b) indicated atomic % values of 24.0, 37.5, and 38.5 for Na, C, and O, respectively. As a result, the precipitated Na_2CO_3 may be used to make an alkaline picrate solution to test for cyanide (see Section 2.2.4). These data support and validate the findings of the ATR–FTIR and XRD analyses.

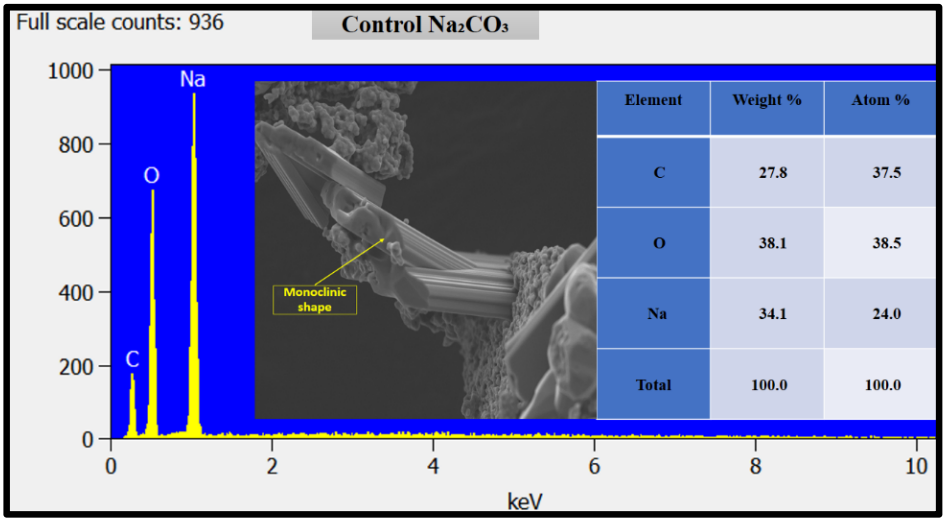

(**a**)

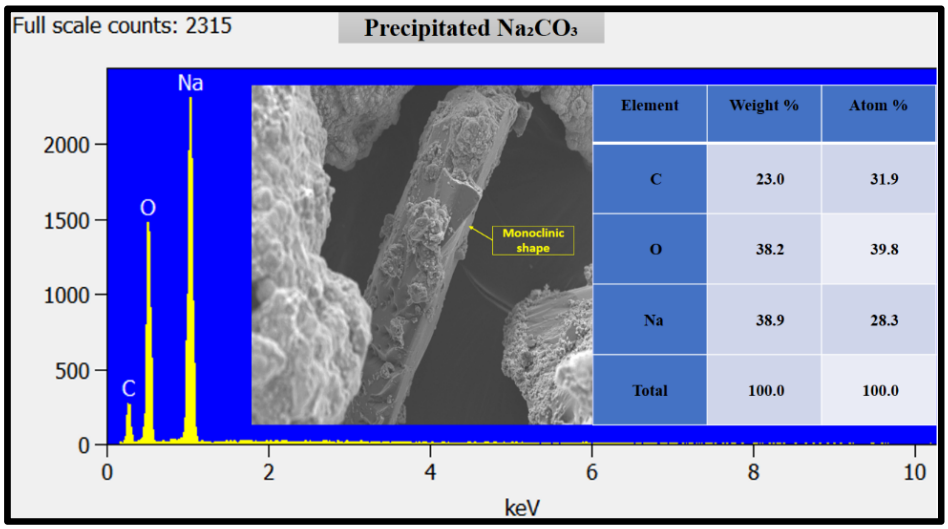

(**b**)

Figure 18. SEM images and EDS spectra of (**a**) control Na_2CO_3 and (**b**) precipitated Na_2CO_3.

4. Conclusions

This paper described the successful production of sodium cyanide (green-NaCN) via the saturation of a NaOH absorbing solution using hydrogen cyanide (HCN) extracted from cassava leaves after 120 min of maceration at 30 °C and 45 min of extraction under vacuum at 35–40 °C. A total of 32.356 g of green-NaCN were produced from 15.70 kg of fresh cassava leaves, representing a percentage yield of 0.21%. The XRD data confirmed the formation of the NaCN crystals having a characteristic cubic structure. The SEM results complemented the latter finding. Moreover, confirming these findings, the EDS data also revealed that the control sample had an aluminium (Al) impurity. The ATR–FTIR results substantiated the synthesis of NaCN crystal, as depicted by a peak at 2090 cm^{-1} which was attributed to C≡N from inorganic cyanides. The obtained results also showed the presence of carbonates (Na_2CO_3 and $NaHCO_3$) and NaOH impurities in both the standard and green-NaCN. Finally, based on the protocol established in this study, it can be concluded that it is possible to synthesise NaCN with minimal carbonate impurities if the following steps are taken: (I) limit the contact time between the NaOH absorbing solution and atmospheric CO_2; (II) continue the saturation process well past the onset of plateauing of the NaCN concentration to decrease the residual NaOH content; (III) dry the NaCN slurry in an inert oven; (IV) degas the Milli-Q water before preparing the homogenate.

Author Contributions: The authors' contributions during the research were as follows: Conceptualization, I.M., V.P., S.M. and O.Z.; Formal analysis, I.M., V.P., S.M. and O.Z.; Investigation, I.M.; Methodology, I.M., V.P., S.M. and O.Z.; Project administration, I.M., V.P., S.M. and O.Z.; Resources, I.M., V.P., S.M. and O.Z.; Supervision, V.P., S.M. and O.Z.; Validation, I.M., V.P., S.M. and O.Z.; Visualization, I.M., V.P., S.M. and O.Z.; Writing—original draft, I.M.; Writing—review and editing, V.P., S.M. and O.Z. All authors have read and agreed to the published version of the manuscript.

Funding: This research received no external funding.

Institutional Review Board Statement: Not applicable.

Informed Consent Statement: Not applicable.

Acknowledgments: The authors wish to extend their gratitude to the Durban University of Technology, the University of Johannesburg and the Council for Scientific and Industrial Research (Pretoria) for the use of their laboratories.

Conflicts of Interest: The authors declare no conflict of interest.

References

1. European Centre for Ecotoxicology and Toxicology of Chemicals. *Cyanides of Hydrogen, Sodium and Potassium, and Acetone Cyanohydrin (CAS No. 74-90-8, 143-33-9, 151-50-8 and 75-86-5)*; ECETOC: Brussels, Belgium, 2007; pp. 13–31.
2. Attahdaniel, B.E.; Ebisike, K.; Adeeyinwo, C.E.; Adetunji, A.R.; Olusunle, S.O.O.; Adewoye, O.O. Production of Sodium Cyanide from Cassava Wastes. *Int. J. Sci. Technol.* **2013**, *2*, 707–709.
3. Gail, E.; Gos, S.; Kulzer, R.; Lorösch, J.; Rubo, A.; Sauer, M.; Kellens, R.; Reddy, J.; Steier, N.; Hasenpusch, W. Cyano Compounds, Inorganic. In *Ullmann's Encyclopedia of Industrial Chemistry*; Wiley-VCH Verlag GmbH & Co. KGaA: Weinheim, Germany, 2011; Volume 10, pp. 673–710.
4. Deepa, H.A.; Raj, A.; Asha, P. Evaluation on Production and Economics of Acrylonitrile by Sohio Process. In Proceedings of the International Conference on Recent Trends in Engineering and Technologies, Mysuru, India, 13 March 2016.
5. Attahdaniel, E.B.; Enwerem, P.O.; Lawrence, P.G.; Ofiwe, C.U.; Olusunle, S.O.O.; Adetunji, A.R. Green synthesis and characterization of sodium cyanide from cassava (Manihot esculenta CRANTZ). *FTSTJ* **2020**, *5*, 247–251.
6. Davis, S.; Murray, J.; Katsiadaki, I. *Cyanide in the Aquatic Environment and Its Metabolism by Fish*; World Class Science for the Marine and Freshwater Environment, Ed.; Centre for Environment Fisheries & Aquaculture Science: Suffolk, UK, 2017; p. 72.
7. Panou, M.; Gkelis, S. Cyano-assassins: Widespread cyanogenic production from cyanobacteria. *bioRxiv* **2020**. [CrossRef]
8. Bhalla, T.C.; Kumar, V.; Kumar, V. Microbial Remediation of Cyanides. In *Bioremediation Current Research and Applications*, 1st ed.; Ashok, D., Rathoure, K., Eds.; IK International: Delhi, India, 2017; p. 23.
9. Ubwa, S.T.; Otache, M.A.; Igbum, G.O.; Shambe, T. Determination of Cyanide Content in Three Sweet Cassava Cultivars in Three Local Government Areas of Benue State, Nigeria. *Food Sci. Nutr.* **2015**, *6*, 1078–1085. [CrossRef]
10. Zuk, M.; Pelc, K.; Szperlik, J.; Sawula, A.; Szopa, J. Metabolism of the Cyanogenic Glucosides in Developing Flax: Metabolic Analysis, and Expression Pattern of Genes. *Metabolites* **2020**, *10*, 288. [CrossRef] [PubMed]
11. Bayitse, R.; Tornyie, F.; Bjerre, A.-B. Cassava cultivation, processing and potential uses in Ghana. In *Handbook on Cassava*; Klein, C., Ed.; Nova Science Publishers, Inc.: Hauppauge, NY, USA, 2017; p. 21.
12. Omotayo, A.R.; EL-Ishaq, A.; Babatunde, A.S. Assessment of cyanide content in white, light yellow and deep yellow cassava Grit (Gari) sold in Damaturu Metropolis. *Am. J. Food Sci. Health* **2015**, *1*, 5.
13. Nyirenda, K.K. Toxicity Potential of Cyanogenic Glycosides in Edible Plants. In *Medical Toxicology*; Erkekoglu, P., Ogawa, T., Eds.; IntechOpen: London, UK, 2021; pp. 1–19.
14. Shackelford, G.E.; Haddaway, N.R.; Usieta, H.O.; Pypers, P.; Petrovan, S.O.; Sutherland, W.J. Cassava farming practices and their agricultural and environmental impacts: A systematic map protocol. *Environ. Evid.* **2018**, *7*, 30. [CrossRef]
15. Spencer, D.S.C.; Ezedinma, C. Cassava cultivation in sub-Saharan Africa. In *Achieving Sustainable Cultivation of Cassava Volume 1*, 1st ed.; Burleigh Dodds Science Publishing: Cambridge, UK, 2017; pp. 123–148.
16. Otekunrin, O.A.; Sawicka, B. Cassava, a 21st Century Staple Crop: How can Nigeria Harness Its Enormous Trade Potentials? *Acta Sci. Agric.* **2019**, *3*, 194–202. [CrossRef]
17. Mudombi, C.R. An Ex-Ante Economic Evaluation of Genetically Modified Cassava in South Africa. Master's Thesis, University of Pretoria, Pretoria, South Africa, 2010.
18. Mabasa, K.G. Epidemiology of Cassava Mosaic Disease and Molecular Characterization of Cassava Mosaic Viruses and Their Associated Whitefly (Bemisia Tabaci) Vector in South Africa. Master's Thesis, University of the Witwatersrand, Johannesburg, South Africa, 2007.
19. Makwarela, M.; Rey, C. Cassava Biotechnology, a southern African perspective. *Biotechnol. Mol. Biol. Rev.* **2006**, *1*, 10.
20. Cuvaca, I.B.; Eash, N.S.; Zivanovic, S.; Lambert, D.M.; Walker, F.; Rustrick, B. Cassava (Manihot esculenta Crantz) Tuber Quality as Measured by Starch and Cyanide (HCN) Affected by Nitrogen, Phosphorus, and Potassium Fertilizer Rates. *J. Agric. Sci.* **2015**, *7*, 36–49. [CrossRef]

21. Srihawong, W.; Kongsil, P.; Petchpoung, K.; Sarobol, E. Effect of genotype, age and soil moisture on cyanogenic glycosides content and root yield in cassava (Manihot esculenta Crantz). *Agric. Nat. Resour.* **2015**, *49*, 13.
22. Brito, V.H.S.; Ramalho, R.T.; Rabacow, A.P.M.; Moreno, S.E.; Cereda, M.P. Colorimetric method for free and potential cyanide analysis of cassava tissue. *Gene Conserve* **2009**, *8*, 1–11.
23. Oshima, H.; Ueno, E.; Saito, I.; Matsumoto, H. Quantitative Determination of Cyanide in Foods by Spectrophotometry using Picric Acid Test Strips. *Jpn. J. Food Chem.* **2003**, *10*, 96–100.
24. Asterion, A. Carbonates in the Plating Bath. Available online: https://asterionstc.com/2016/06/carbonates-plating-bath/ (accessed on 22 July 2021).
25. Dusica, I.; Bojana, K.; Tea, B.; Radmilo, C.; Djuro, V.; Jovanka, L.; Slavica, S. Effect of microwave heating on content of cyanogenic glycosides in linseed. *Ratar. Povrt.* **2012**, *49*, 63–68. [CrossRef]
26. Castada, H.Z.; Liu, J.; Ann Barringer, S.; Huang, X. Cyanogenesis in Macadamia and Direct Analysis of Hydrogen Cyanide in Macadamia Flowers, Leaves, Husks, and Nuts Using Selected Ion Flow Tube-Mass Spectrometry. *Foods* **2020**, *9*, 174. [CrossRef] [PubMed]
27. Nandiyanto, A.B.D.; Oktiani, R.; Ragadhita, R. How to Read and Interpret FTIR Spectroscope of Organic Material. *Indones. J. Sci. Technol.* **2019**, *4*, 97–118. [CrossRef]
28. Tesleva, E.P.; Gil, L.B.; Solovyan, A.V. Thermodeformational Behavior of Cubic Crystals of Sodium Cyanide. In Proceedings of the VII International Scientific Practical Conference "Innovative Technologies in Engineering", Yurga, Russia, 19–21 May 2016.